Ecological Engineering 119 (2018) 97–108

Contents lists available at ScienceDirect

Ecological Engineering

journal homepage: www.elsevier.com/locate/ecoleng

Coupled hydrodynamic and water quality simulation of algal bloom in the Three Gorges Reservoir, China

Jian Li[a,*], Wenjun Yang[b], Wenjie Li[c], Lin Mu[a], Zhongwu Jin[b]

[a] College of Marine Science and Technology, China University of Geosciences (Wuhan), No. 388 Lumo Road, Wuhan 430074, China
[b] Changjiang River Scientific Research Institute, No.23 Huangpu Road, Wuhan 430010, China
[c] National Inland Waterway Regulation Engineering Research Center, Chongqing Jiaotong University, Chongqing 400074, China

ARTICLE INFO

Keywords:
SELFE
WASP
CANDI
Algal bloom
Three Gorges Reservoir

ABSTRACT

Patterns of spatial and temporal variability of algal bloom in the Three Gorges Reservoir (TGR) of China were investigated using Semi-implicit Eulerian-Lagrangian Finite Element (SELFE) model, an unstructured grid, 3-dimensional, hydrodynamic model fully coupled with an extended version of Water Quality Analysis Program (WASP) and the Carbon and Nutrients DIagenesis (CANDI) model. The coupled model was driven by the discharge, operational water level of the TGR, nutrients and phytoplankton from the upstream, climate condition included the solar radiation, heat fluxes and precipitation observed in the hydrometric and meteorological stations. The simulations were conducted to study the dynamic process of the algal blooms occurred in September 2007 and June 2008, and the modeling results agreed well with the field data included nutrients, chlorophyll-a concentrations in the TGR. The results indicated that the nutrients and chlorophyll-a concentrations showed obvious difference in the mainstream and the tributaries affected by the diurnal evolution of the phytoplankton during the algal bloom period. The location of algal bloom in the tributary Xiangxi River where the maximum chlorophyll-a concentration was greater than 30 μg/L was about 20 km from the river mouth, which coincided with the position of backwater tail controlled by the operation of the TGR. Meanwhile, the nutrients concentration near the river bed reached nearly 10 times of the concentration near the water surface after considering the nutrients released from the re-suspended sediment and the biogeochemical process in the river bed sediment. Finally, the climate change affected the aquatic ecosystem in the TGR was investigated and the countermeasure to inhibit the algal bloom in the tributary was suggested through the scenario modeling.

1. Introduction

The construction of the Three Gorges Reservoir (TGR) and cascaded reservoirs in the upper reach of the Yangtze River obstructed the natural waterways and has allowed a large volume of water storage since 2003 (Stone, 2008). The water impounding of the TGR decreased the flow velocity and the clearing capability in the Yangtze River. This is particularly the case in tributaries as a result of the backwater blocking effect, which has caused many water quality problems in the tributaries of the TGR in recent years (Yang et al., 2010; Liu et al., 2012; Zhou et al., 2015). The flow becomes nearly motionless in the tributaries and mixed with the nutrients released from chemical factories, which has led to the rapid reproduction of phytoplankton included diatoms and blue-green algae over a short time that's known as the algal bloom (Ye et al., 2006; Zheng et al., 2011).

In recent years, many numerical simulation research studies have been conducted in the TGR and its tributaries, such as the 1-dimensional modeling (Wang et al., 2009; Huang et al., 2015a,b), laterally-averaged 2-dimensional modeling (Dai et al., 2013; Ma et al., 2015), 3-dimensional modeling (Li et al., 2012, 2014), and also the non-point pollution modeling by distributed hydrological model (Hormann et al., 2009). The 1-dimensional model can only give the information about the water quality evolution at the longitudinal line of the river, and the physical variables cycling processes must be simplified. The laterally-averaged 2-dimensional model can consider the physical variables cycling in the longitudinal profile along the river course and the important factors affecting the growth of the phytoplankton in the water column, but the mass transport at the cross section cannot be simulated. The evolution of the aquatic ecosystem performs obvious 3-dimensional characteristics (Xu et al., 2009), so the 3-dimensional model was deemed to be necessary to describe the dynamic evolution process of the ecosystem in the TGR (Li et al., 2014). Additionally, the mass exchange between the Yangtze River mainstream and the tributaries (Ma et al., 2015) and the mass exchange

* Corresponding author.
E-mail address: lijian_cky@hotmail.com (J. Li).

https://doi.org/10.1016/j.ecoleng.2018.05.018
Received 13 July 2017; Received in revised form 4 May 2018; Accepted 14 May 2018
Available online 26 May 2018

between the overlying water and the interstitial water in the river bed sediment (Huang et al., 2015a,b) both affect the water quality in the TGR. The first mass exchange process was considered in the laterally-averaged 2-dimensional modeling (Dai et al., 2013; Ma et al., 2015), but only a tributary was modeled and the plug flow position at the confluence zone was artificially setup, which cannot consider the real physical flow condition, this problem must be solved through 3-dimensional modeling the TGR area includes the Yangtze River mainstream and the tributaries. The second mass exchange process involved the nutrients diffusion induced by the re-suspension of the sediment in the river bed (Huang et al., 2015a,b) and the biogeochemical reaction process in the interstitial water (Hipsey, 2015), which has been studied by the flume experiment considering the TGR situation (Huang et al., 2015a,b) and considered in the 1-dimensional model (Huang et al., 2015a,b). Until now, most of the water quality studies about the TGR come from the field data analysis at sampling points (Xu et al., 2009; Ji et al., 2010), catchment-scaled mass transport flux analysis (Zhou et al., 2015) and the 1-dimensional and 2-dimensional modeling, the temporal and 3-dimensionally spatial evolution of the water quality state variables in the TGR and the interaction among the flow, air, sediment, nutrients and phytoplankton are still not clearly understood. So, 3-dimensional model considering the physical-chemical-biological dynamic processes should be developed to study the dynamic evolution of the algal bloom in the TGR.

At the other side, the mesh structure used in the 3D model can be divided into structured and unstructured mesh (Li et al., 2014); models based on structured mesh have a simple data structure and can be easily programmed, hence most of the hydrodynamic and water quality models used this approach (Jia et al., 2013; Ben and Chris, 2015). However, the structured-mesh model has the disadvantage that cannot capture the complex geometric boundary line of the river, lake or estuary, which will introduce inaccuracies in modeling caused by the zigzag meshing boundary (Ferziger and Peric, 2002). The other challenge is that the complex terrain of the river bed also affects the modeling accuracy to a certain extent (Ferziger and Peric, 2002). These years the unstructured-mesh models with the terrain-following vertical coordinate system (Zhang et al., 2016) can tackle the aforementioned problems and have been widely used in the water quality modeling research (Justic and Wang, 2014; Ye et al., 2016). Therefore, the water quality model considering the aforementioned important physical-chemical processes was developed in the framework of Water quality Analysis Simulation Program (WASP) (Wool et al., 2008), and coupled with the biogeochemical model called Carbon and Nutrients DIagenesis (CANDI) (Luff and Moll, 2004) and the widely used 3D unstructured mesh hydrodynamic Semi-implicit Euler-Lagrange Finite Element model (SELFE) (Zhang and Baptista, 2008), the coupled model was applied to study the algal bloom problem in the TGR with all the aforementioned characteristics.

Firstly, the principles of the coupled hydrodynamic and water quality model will be introduced, especially the water quality related with the suspended sediment in the water column and the biogeochemical process in the river bed sediment. Then, the coupled model was applied to simulate the dynamic evolution processes of algal blooms occurring in the TGR area near the dam. Finally, the climate change scenarios in the future affected the aquatic ecology system in the TGR were predicted through numerical modeling and the countermeasure to inhibit the algal bloom problem in the tributaries was suggested.

2. Methodology

The coupled hydrodynamic and water quality model integrates SELFE (Zhang and Baptista, 2008), WASP 6.0 (Wool et al., 2008) and CANDI (Luff and Moll, 2004) into a general framework as shown in Fig. 1. The principles of the WASP and CANDI models can be found in the literatures (Wool et al., 2008; Luff and Moll, 2004). Additionally, some important modules have been added to WASP6.0, leading to an extended version of WASP (EWASP), which will be introduced in the following sections.

2.1. Hydrodynamics module

The water quality model was driven by the hydrodynamic model SELFE, which is a widely used unstructured grid coastal ocean circulation model (Zhang and Baptista, 2008) that has been applied to simulate many cross-scaled fluid phenomena from creeks to oceans (Ye et al., 2016). This prognostic model employs the generic length turbulent closure model including k-ε, k-ω and some other high-order turbulent closure schemes for modeling the vertical hydrodynamic mixing and the wave function for calculating the free surface fluctuation. The SELFE model uses the Eulerian-Lagrangian Method (ELM) for the advection term calculation in the horizontal moment equations with unstructured-grid finite-element method, which can increase the simulation efficiency (Wang et al., 2008). The users can choose the low order upwind scheme or the second-order Total Variational Diminish (TVD) scheme to discretize the scalar equations considering the accuracy and simulation efficiency. It's noted that the TVD scheme can ensure mass conservation of the scalar quantities (Wang et al., 2008), which means that the large mass concentration gradient can be captured accurately. Unstructured triangular mesh used in SELFE with the interpolation of the high-resolution digital elevation data (10 m raster cell size), which can fit the zigzag boundary lines and the complex river bed terrain in the TGR followed by the pure "S" coordinate system (Zhang and Baptista, 2008; Li et al., 2012).

2.2. Water quality module

The water quality model used to study the algal bloom problem in the TGR was initially developed based upon WASP6.0 (Wool et al., 2008; Li et al., 2012) and adapted from the most updated WASP version (Justic and Wang, 2014), which leads to the extended version of WASP called EWASP and includes several substantial modifications following the field data analyses and modeling results about TGR water quality problem (Xu et al., 2009; Ji et al., 2010; Jia et al., 2013; Li et al., 2014; Ma et al., 2015).

The major advantages of EWASP include: (1) the mass exchange between overlying water and interstitial water in river beds under turbulent diffusion effects in the boundary layer; (2) dynamic sediment biogeochemical modeling which considers the interstitial water advection, bio-disturbance, physical characteristics of sediment; (3) formulations for calculating oxygen re-aeration induced by both wind and flowing stress which is suitable for calculating the re-aeration in mountainous river conditions; (4) aerodynamic bulk model calculating the heat exchange between atmosphere and water column considering different components of solar radiance and also the vertical underwater light intensity influencing the benthic photosynthesis; and (5) consideration of the re-suspension of river bed sediment, which increases light attenuation limiting the benthic phytoplankton growth in the shallow water zone.

The free surface elevation, flow velocity and other turbulent variables calculated by SELFE were the inputs for EWASP and CANDI. The oxygen in the atmosphere can penetrate into water column through turbulent diffusion (Chu and Jirka, 2003), and heat exchange will also occur between the atmosphere and water column through solar irradiance calculated by the bulk aerodynamic model (Zeng et al., 1998). The EWASP model is the core module of the integrated water quality modeling system, of which the component variables and the interaction relationship can be seen in Fig. 1. The EWASP model has ten state variables including ammonia (NH_4), nitrate (NO_3), organic nitrogen (ON), phosphate (PO_4), organic phosphorous (OP), dissolved oxygen (DO), carbonaceous biochemical oxygen demand (CBOD), carbonate equivalent (PHY) and chlorophyll-a (CHL) representing the

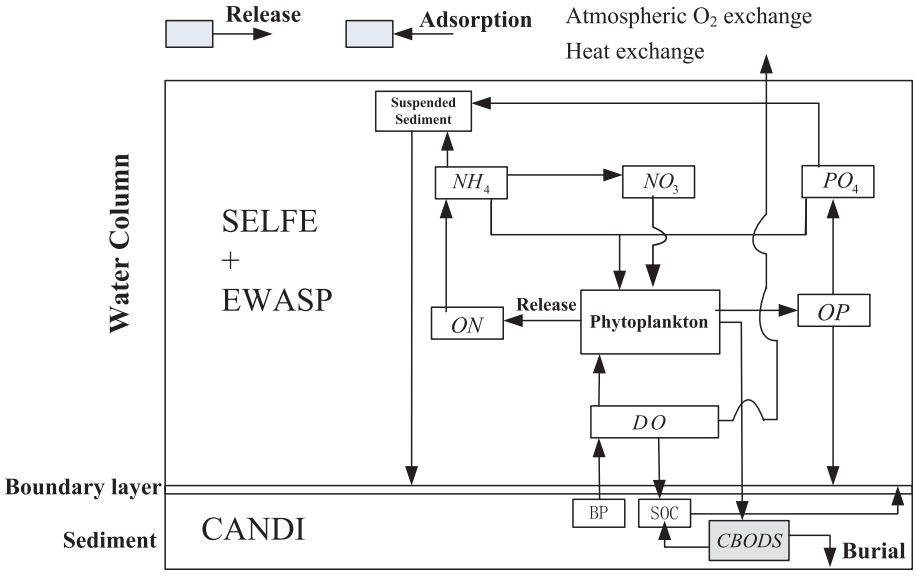

Fig. 1. Schematics of the coupled hydrodynamic and water quality model.

phytoplankton biomass and suspended sediment (SSED). The state variables used in the water quality modeling considered the local aquatic ecological characteristics and the available field data in the TGR case study. More state variables will increase the modeling capability to represent aquatic ecology but also the simulation uncertainty, so some biogeochemical modules were simplified and some have been refined in EWASP compared with WASP6.0.

All the conservation of mass of the scalar variables were represented and solved using the typical advection–diffusion–reaction equation (Zhang and Baptista, 2008):

$$\frac{\partial C_i}{\partial t} + \frac{\partial (uC_i)}{\partial x} + \frac{\partial (vC_i)}{\partial y} + \frac{\partial (wC_i)}{\partial z} = K_h\left(\frac{\partial^2 C_i}{\partial x^2} + \frac{\partial^2 C_i}{\partial y^2}\right) + K_v \frac{\partial^2 C_i}{\partial z^2} + S_i + B_i \quad (1)$$

where u, v and w are velocity components corresponding to the x, y and z coordinates in the Cartesian coordinate system; K_h and K_v are the horizontal and vertical eddy diffusivity, respectively; C_i [i = 1,…,10] is the mass concentration; S_i [i = 1,…,10] is the sum of internal biochemical sources and sinks for each of the ten state variables including S_{DO} (dissolved oxygen), S_{PHY} (phytoplankton biomass represented by carbon), S_{CHL} (phytoplankton biomass representing by chlorophyll-a), S_{CBODW} (carbonaceous biochemical oxygen demand in water column), S_{NH4} (ammonia), S_{NO3} (nitrate), S_{ON} (organic nitrogen), S_{PO4} (phosphate), S_{OP} (organic phosphorus), and S_{SSED} (suspended sediment); and B_i [i = 1,…,10] denotes the external loading from the open boundary including the XXR, Gaolan River and Yangtze River for each of the ten state variables in the water column listed above.

The aforementioned advection-diffusion-reaction equation can be solved by the transport equation solver in SELFE. The biological processes in EWASP are calculated as the source or sink terms into the transport equation in SELFE, which will be introduced in the following sections. Meanwhile, only the dynamics of DO, suspended sediment and phytoplankton will be introduced because some more factors were considered in the source/sink term, the equations describing the dynamics of another state variables can be found in the manual of WASP (Wool et al., 2008; Justic and Wang, 2014).

2.2.1. Dynamics of DO

The dynamics of DO can be described by the relation of re-aeration, CBOD oxidation, nitrification, phytoplankton respiration, phytoplankton photosynthesis, benthic photosynthesis, and sediment oxygen consumption (Justic and Wang, 2014). The newly added re-aeration caused by wind and high flow velocities in the mountainous rivers in the TGR are described below.

Many empirical formulas calculating the re-aeration coefficient k_w and k_q were given based on the laboratory and field data, but most were calibrated in low flow velocities and are thus not suitable for the TGR case. The oxygen re-aeration formula (Eq. (2)) induced by the combined effects of wind and flow velocity was updated in EWASP (Chu and Jirka, 2003):

$$k_{ge} = Sc^{-2/3}\cdot\left(\frac{\nu}{2\cdot u_*\cdot R_{g-t}}\right)^{1/3}\varepsilon^{1/3} \quad (2)$$

where Sc is the Schmidt number, u_* is the friction velocity; $R_{g\text{-}t}$ is the oxygen-transfer Reynolds number ($R_{g\text{-}t}$ = 0.75); and ε is the turbulent dissipation rate near water surface, which was calculated by SELFE.

2.2.2. Dynamics of suspended sediment

(1) Settling of suspended sediment

The suspended sediment flushed into the TGR decreased and the suspended sediment diameter showed a uniform changing trend in recent years (Jia et al., 2013). Therefore, the median diameter (d_{50}) was used to calculate the settling velocity of the suspended sediment:

$$S_{SSED} = -\omega_{ss}\frac{\partial C_{SSED}}{\partial z} \quad (3)$$

where w_{ss} is the settling velocity (m/s) and C_{SSED} is the suspended sediment concentration (kg/m^3).The settling velocity of suspended sediment w_{ss} can be calculated using Wang's formula calibrated by the experimental and field observed data of fine sediment settling down (Jia et al., 2013):

$$w_{ss} = -9\frac{\nu}{d_{50}} + \sqrt{\left(9\frac{\nu}{d_{50}}\right)^2 + \frac{\gamma_s - \gamma}{\gamma}gd_{50}} \quad (4)$$

where d_{50} is the median diameter (m); ν is the kinematic viscosity of water (m^2/s^2); and γ and γ_s are bulk weight of water and sediment (kg/m^3), respectively.

(2) Interaction between nutrients and suspended sediment

The nutrients included nitrogen and phosphorous interacted with suspended sediment and divided into dissolved and particulate

components. The particulate nutrients settle down with the sediment which accumulated in the bed sediment, whereas the dissolved nutrients are absorbed or released by phytoplankton cells and also transport with the flow. The adsorption of nutrients with suspended sediment was described by a linear isotherm in WASP6.0 (Wool et al., 2008), which cannot be used for the condition of high suspended sediment concentration. The formula (Eq. 5) deduced by Chao et al. (2007) was based on the Langmuir equilibrium isotherm equation, which was suitable for TGR (Li et al., 2014) and was added into WASP.

$$C_p = \frac{1}{2}\left[\left(C_0 + \frac{1}{K_{ads}} + C_{SSED}Q_{\max}\right) - \sqrt{\left(C_0 + \frac{1}{K_{ads}} - C_{SSED}Q_{\max}\right)^2 + \frac{4C_{SSED}Q_{\max}}{K_{ads}}}\right] \quad (5a)$$

$$C_d = \frac{1}{2}\left[\left(C_0 - \frac{1}{K_{ads}} - C_{SSED}Q_{\max}\right) + \sqrt{\left(C_0 + \frac{1}{K_{ads}} - C_{SSED}Q_{\max}\right)^2 + \frac{4C_{SSED}Q_{\max}}{K_{ads}}}\right] \quad (5b)$$

where C_d and C_p are the dissolved and particulate nutrients concentration after the adsorption reach equilibrium (mg/L), respectively; C_0 is the initial nutrient concentrations at every time step in the solution (mg/L); K_{ads} is the adsorption constants (mg/L); and Q_{max} is the maximum adsorption capability (unitless).

2.2.3. Dynamics of phytoplankton

The dynamics of phytoplankton expressed in carbon equivalents can be described by the following equation (Justic and Wang, 2014):

$$S_{PHY} = (G_p - D_p)C_{PHY} - w_{PHY}\frac{\partial C_{PHY}}{\partial z} \quad (6)$$

where G_p and D_p are the growth rate and death rate of phytoplankton, respectively (day^{-1}); w_{PHY} is the settling velocity of phytoplankton (m/day); and $\frac{\partial C_{PHY}}{\partial z}$ is the vertical gradient concentration.

Most functions for calculating the growth rate G_p, the death rate D_p and the settling term were the same as those used in the updated WASP model (Justic and Wang, 2014). Only the terms and functions associated with modeling the phytoplankton in the TGR and the tributaries were added here and are introduced below.

Firstly, the suspended sediment increased the light attenuation in the water column due to the high suspended sediment concentration occurring in the flooding season, particularly in the tributaries, was considered in EWASP. The light attenuation caused by the water, phytoplankton, the suspended sediment, and the re-suspended sediment near river bed due to the shear stress was considered. The light intensity decay in the water column was calculated by the combined attenuation coefficient K_e as:

$$K_e = K_0 + K_{chl} + K_{SS} + K_{sr} \quad (7)$$

where K_0, K_{chl} and K_{SS} are the light attenuation coefficient caused by pure water background, phytoplankton cells, and suspended sediment shading (m^{-1}), respectively; and K_{sr} is the benthic light attenuation due to sediment re-suspension at the river bed.

The last three terms in Eq. (7) were calculated as:

$$K_{chl} = K_C C_{CHL} \quad (8a)$$

$$K_{SS} = K_S C_{SSED} \quad (8b)$$

$$K_{sr} = k_\tau^{(\tau_b - \tau_{ce})} \quad (8c)$$

where, K_c, K_S, k_τ, τ_b and τ_{ce} are all empirical parameters, which should be calibrated by the available field observed data in the TGR.Secondly, the river flow can inhibit the phytoplankton growth because of turbulent mixing, nutrients dilute and transport, but little knowledge about the mechanism of inhibition effect has been obtained. The flow limitation factor f_U was used in EWASP to characterize the limitation effect as (Li et al., 2012, 2014):

$$f_U = 0.7^{6.6U} \quad (9)$$

where U is the flow velocity (m/s).

2.3. Biogeochemical module

The biogeochemical reaction occurs in the interstitial water after some nutrients and phytoplankton settled down to the bed as shown in Fig. 1, which is similar to the cycling and reaction in the water column. Then, the biogeochemical model CANDI was coupled with the SELFE and EWASP model as shown in Fig. 1 and the mass exchange at the water-sediment interface was calculate following the Fick law considering the turbulent diffusion. The default values of the parameters in CANDI related with the DO, nutrients, organic and inorganic matters were used, which should be calibrated by the field data of TGR in the future study.

3. Application of the coupled model

3.1. Modeling area

The TGR is located in Hubei and Chongqing Province of China and

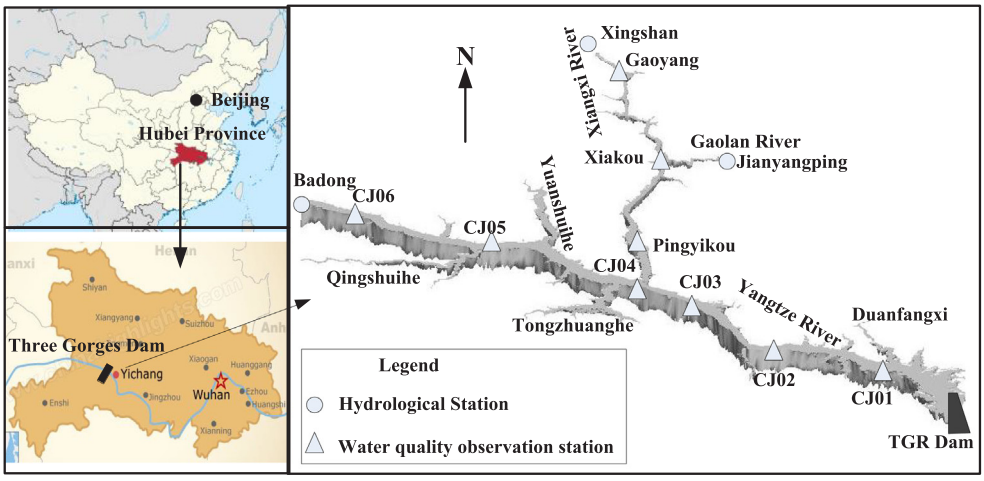

Fig. 2. Three Gorges Reservoir and in-situ sampling points.

the total backwater length is about 670 km, but only the area near the dam in Yichang, Hubei Province was studied as shown in Fig. 2. The XXR is an important tributary in the TGR; water quality change was observed in XXR when algal bloom occurred from 2003 to 2009 (Xu et al., 2009). Many different sized tributaries exist in the TGR along the Yangtze River in Fig. 2. Although algal bloom problems have occurred in many tributaries such as the Tongzhuang River and Yuanshui River, there are no hydrological stations in these tributaries and the inflow discharge was smaller than that in the XXR (Ma et al., 2015), thus all tributaries except XXR were seen as closed bay without inflow from upstream (See Fig. 2).

The simulation of the algal bloom in XXR has already been conducted without considering the Yangtze River mainstream flow and the local hydrodynamics at the confluence affecting the mass exchange (Li et al., 2012, 2014). In this study, the waterways included the mainstream and the tributaries were simulated considering the backwater effect of TGR operation. A total of 11 and 6 water quality observation stations were arranged in the XXR and Yangtze River mainstream for observing the water quality state variables during the algal bloom period (Yang et al., 2010) as seen in Fig. 2. There are also 5 hydrological stations recording the discharge and water table in the TGR area and 2 meteorological stations in Xingshan and Yichang in Fig. 3, which supply the field data for the necessary inputs for the coupled modeling.

3.2. Modeling setup

The TGR area includes the Yangtze River mainstream and the tributaries was discretized as 122,988 triangular mesh and 30 pure "S" vertical coordinates layers were used to create the 3-dimensional calculation domain, which leads to nearly 3.69 million prism control volumes. The flow and mass transport were solved through MPI (Message Passage Interface) parallelization of SELFE model. The calculation time step was set as 1.0 s following the Courant-Friedrichs-Lewy (CFL) condition (Ferziger and Peric, 2002). The refined mesh size and relatively short time step were necessary to describe the local vortex structure at the confluence zone between the Yangtze River mainstream and the tributaries in Fig. 4 and the unsteady diurnal changing process of the nutrients concentration and the biomass of phytoplankton during the period of algal bloom in the TGR as seen in Figs. 5 and 6. Although the parallelization of the hydrodynamic model SELFE was conducted, the water quality and biogeochemical models were still running on the serial computational mode, modeling 1 time of algal bloom in TGR should cost 5 days. This will limit the simulated period of the water quality process, but it's long enough to capture the quick evolutional process of algal bloom in the TGR, which generally lasts for fewer than 2 months from outbreak to ending (Xu et al., 2009). The boundary and initial conditions of hydrodynamics, suspended sediment, nutrients, chlorophyll, and other state variables in the TGR were set up based on the field data (Ji et al., 2010). The Badong, Xingshan, and Jianyangpin stations were seen as the inlets and the dam was the outlet with fluctuated water level as shown in Fig. 2, which was the same with the unsteady process setting in the literatures (Li et al., 2012, 2014).

The weather data recorded at the Xingshan and Yichang Meteorological Observation Stations were downloaded from the China Meteorological Data Sharing Service System, which was used in the calibration and prediction of the water quality modeling. The weather data from September 25th, 2007 to October 16th, 2007 showed the air temperature fluctuated from 20 °C to 30 °C and the long-wave solar radiance changed around 600 W/m^2. These factors both provided favorable conditions for the evolution of algal bloom. In addition, the precipitation could decrease the air temperature, which can inhibit the growth of phytoplankton. This leads to a complex correlation between the algal bloom and the weather condition. Moreover, the local weather condition in the TGR have shown a close relation with the development of an algal bloom, which has been observed and analyzed in previous researches (Hormann et al., 2009; Li et al., 2015; Zheng et al., 2011) and will be also studied using the coupled model in Section 4.

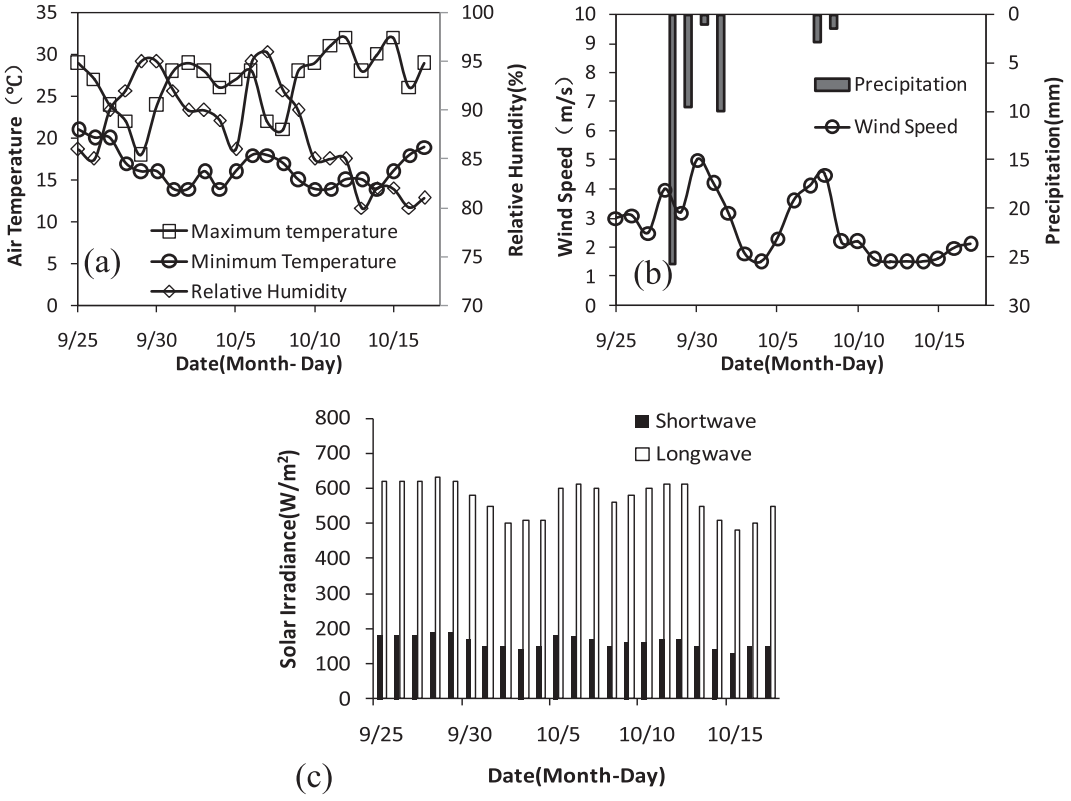

Fig. 3. The field data at Xingshan Meteorological Station ((a) air temperature and relative humidity; (b) wind speed and precipitation; and (c) solar radiance).

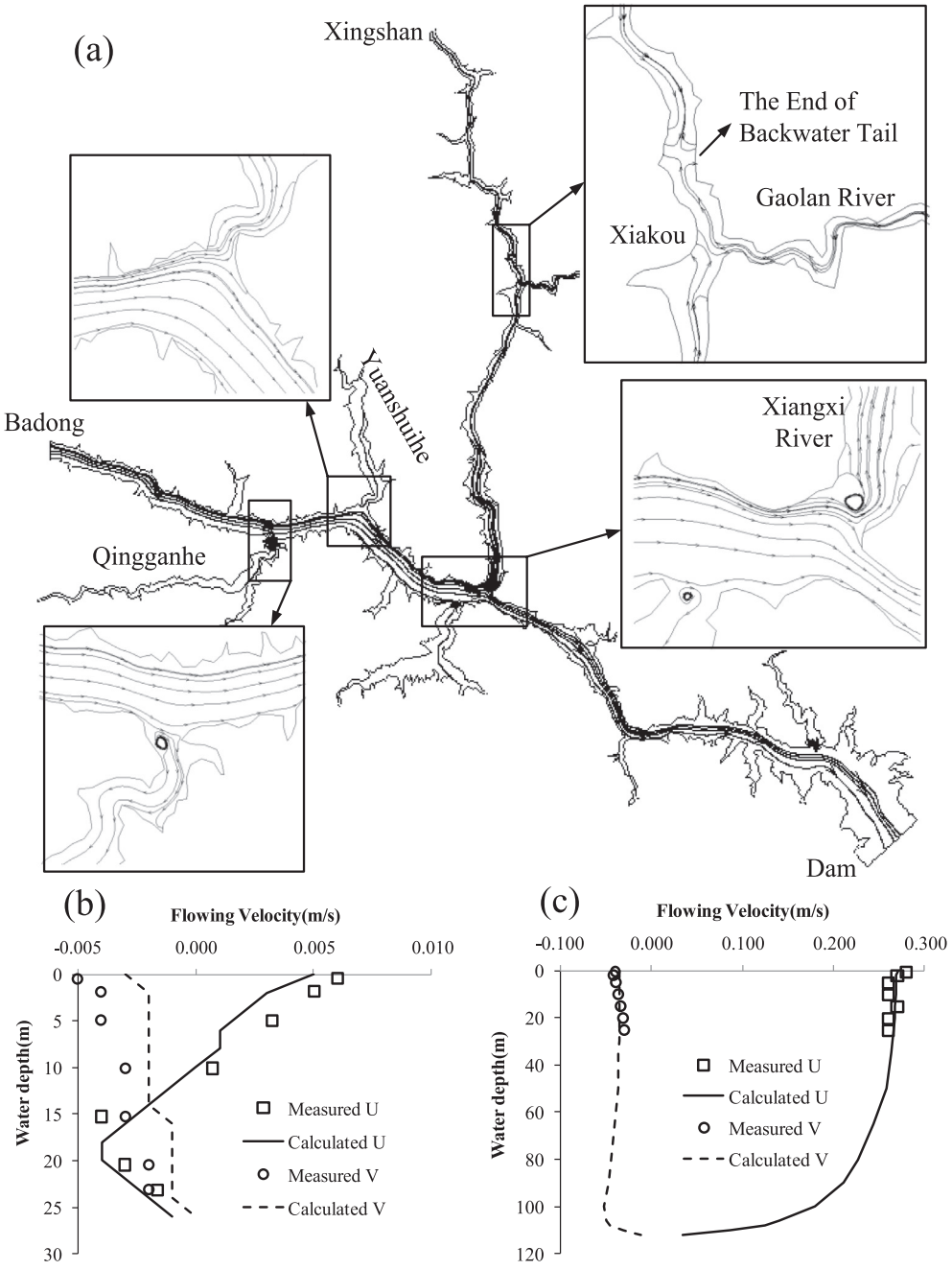

Fig. 4. Calculated streamlines and flow velocity in the TGR ((a) streamlines; (b) flow velocity at Xiakou; and (c) flow velocity at CJ04).

3.3. Calibration

Calibration of the coupled SELFE-EWASP model will be conducted to check the calculation accuracy of hydrodynamics, nutrients and chlorophyll-a compared with the observed data. The comparisons of the other state variables included DO, CBOD and suspended sediment between calculation and observations will not be shown here.

(1) Hydrodynamics

The flow field at the confluence of XXR and Yangtze River was complex because of the interaction between flows from different directions, which affects the suspended sediment, nutrients and phytoplankton transport in the tributaries (Fig. 4(a)). Moreover, the end of backwater tail in the XXR and the vortex formed at the confluence can be observed in Fig. 4(a).

The flow velocity measured with an acoustic Doppler velocimeter (ADV) during the period of algal bloom (Ji et al., 2010; Ma et al., 2015) was used to check the hydrodynamic calculation accuracy. The measured and calculated flow velocity at Xiakou showed the water body became nearly static during the algal bloom period with a flow velocity generally smaller than 0.005 m/s (Fig. 4(b)). Moreover, the longitudinal flow velocity was positive near the water surface while negative under 10 m water depth, which indicated that the water body near surface flowed downstream but flowed upstream near the river bed in the XXR, which has previously been observed using Acoustic Doppler Velocimeter (ADV) and flow visualization technique (Ji et al., 2010; Ma et al., 2015). The flow velocity in the Yangtze River was 0.2–0.3 m/s along most of the water depth at CJ04 (Fig. 4(c)) but the transversal flow velocity was about −0.05 m/s, indicating that the water was flowing back into the XXR at the water impounding stage of the TGR. Moreover, the relatively high flow velocity in the Yangtze River

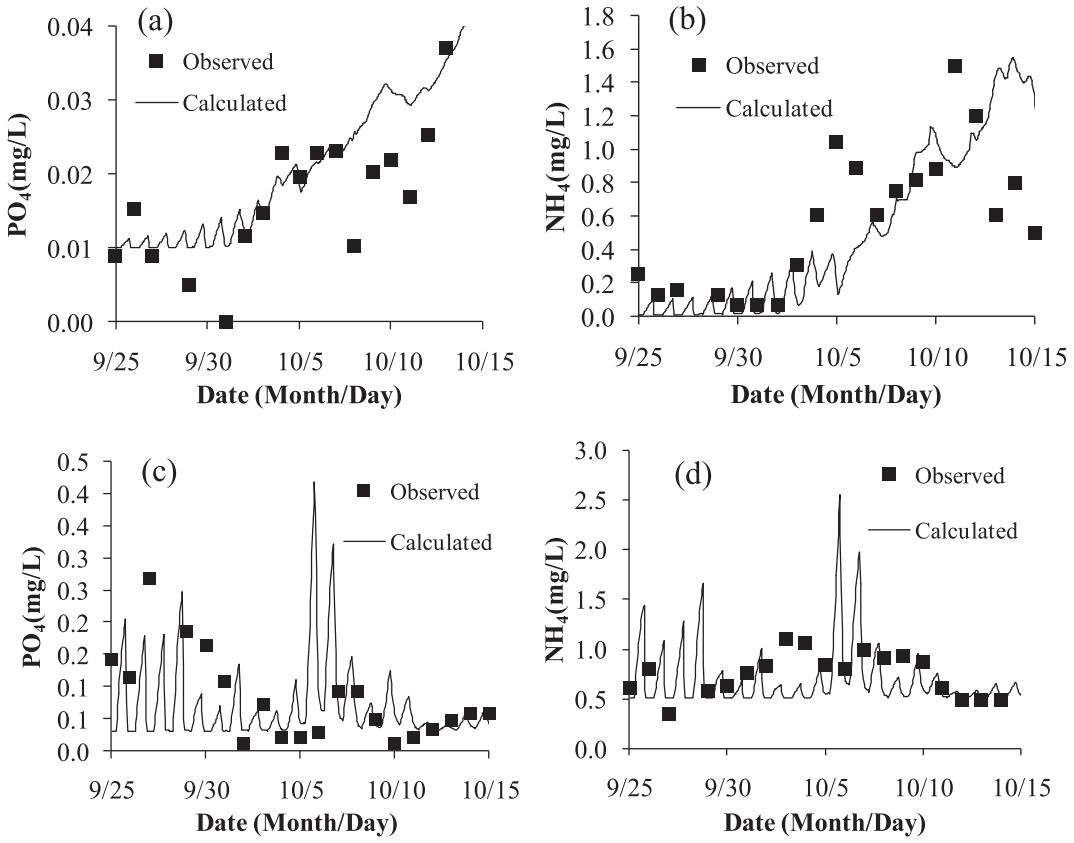

Fig. 5. Comparison of nutrients between calculation and observation in calibration ((a) PO_4 at Xiakou; (b) NH_4 at Xiakou; (c) PO_4 at Gaoyang; and (d) NH_4 at Gaoyang).

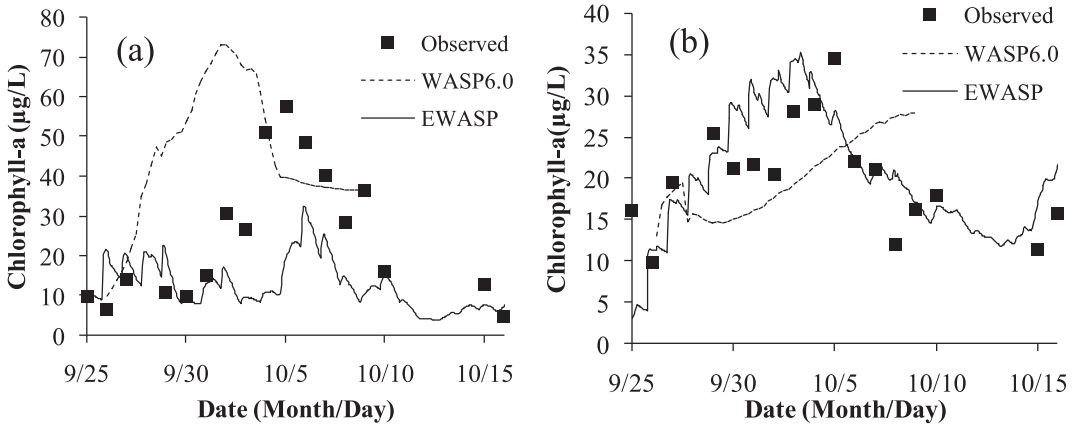

Fig. 6. Comparison of measured and calculated chlorophyll-a concentration ((a) Gaoyang and (b) CJ04).

increased the advection transportation of phytoplankton, which showed good water quality. In contrast, the nearly static hydrodynamic conditions in the tributaries were the main factor causing the algal bloom. The SELFE model can simulate the complex hydrodynamic field in the TGR well and supply an accurate input for water quality modeling.

(2) Nutrients

The observed data of NH_4 and PO_4 at Xiakou and Gaoyang were chosen to show the calibrated results and accuracy to reproduce the algal bloom in the XXR. The PO_4 and NH_4 contents increased at Xiakou from nearly zero to 0.04 and 1.60 mg/L, respectively (Fig. 5(a) and (b)). The NH_4 content at Xiakou began to decrease on October 14th, 2007 (Fig. 5(b)), but NH_4 at Gaoyang (Fig. 5(d)) showed a similar change process with PO_4 (Fig. 5(c)). The nutrient concentrations showed greater fluctuation at Gaoyang than that at Xiakou and were both affected by the diurnal variation of phytoplankton biomass, which cannot be seen from the observational data because of the low observed frequency (1 time per day). The nutrients at Xiakou were influenced by the local growth and death of phytoplankton, whereas the nutrients at Gaoyang were more influenced by the nutrient from upstream.

(3) Chlorophyll-a

The concentration of chlorophyll-a can be used to characterize the biomass of phytoplankton to diagnose the algal bloom. The calculation by the SELFE-EWASP coupled model was compared with the model results by ELCIRC-WASP6.0 (Li et al., 2012) to uncover the advantages

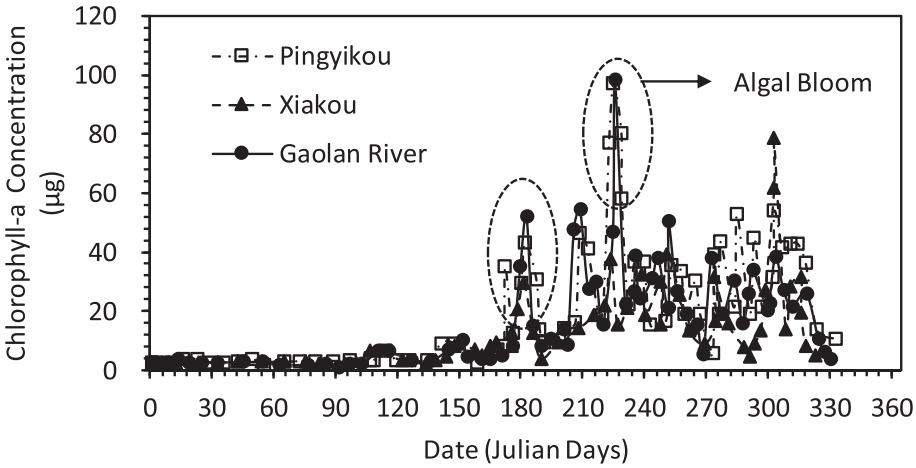

Fig. 7. Long-time observation of the Chlorophyll-a concentration from October 2008 to September 2009.

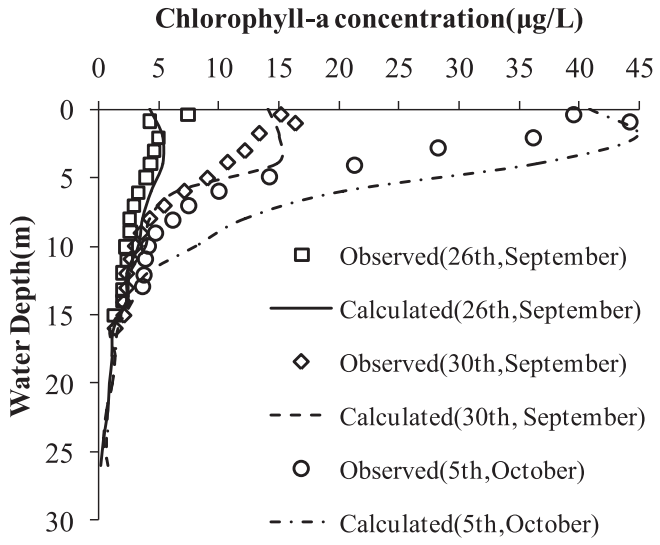

Fig. 8. The vertical profile of chlorophyll-a concentration at Xiakou Station.

Table 1
Major calibration parameters used in the EWASP model.

Symbol	Value	Unit
h_b	From SELFE	m
k_r	1.2	Unitless
τ_b	From SELFE	N/m^2
τ_{ce}	0.005	N/m^2
k_{ge}	Eq. (2)	Unitless
θ_{ge}	1.028	Unitless
γ_s	2650.0	kg/m^3
K_{ads}	0.15	mg/L
Q_{max}	0.584	Unitless
C_d	Eq. 5(a)	mg/L
C_p	Eq. 5(b)	mg/L
K_e	Eq. (7)	m^{-1}
K_w	0.1526	m^{-1}
K_c	0.0088	m^{-1}
K_{sr}	Eq. 8(c)	m^{-1}

and disadvantages of SELFE-EWASP.

SELFE-EWASP can reproduce the changing process of chlorophyll-a included the peak value and the occurrence time more accurately than ELCIRC-WASP6.0 in Fig. 6(a) and (b), and the fluctuation of chlorophyll-a concentration responded to the change of PO_4 and NH_4 at both Gaoyang and Xiakou. Moreover, the chlorophyll-a concentration at Gaoyang and Xiakou reached the maximum value around October 7th and October 5th, 2007, respectively, which indicated the phytoplankton reproduced rapidly. The diurnal fluctuation of chlorophyll and nutrient concentrations can also be seen in Fig. 6, which should be further checked by more frequent field observations, but ELCIRC-WASP6.0 cannot simulate the fluctuation of chlorophyll-a without considering the diurnal change of the solar radiance affecting the photosynthesis of the phytoplankton (Li et al., 2012).

Two kinds of field observation on the evolution of the water quality and the phytoplankton biomass in the typical tributaries included XXR and the Yangtze River mainstream were conducted until now, which included long time observation with low sampling frequency as shown in Fig. 7 (1 time per month lasted for 1 year) and short time observation with high sampling frequency in this research. The long-time observation serves for understanding the seasonal variation of the water quality in the TGR, and the short time observation mainly serves for understanding the dynamic process of the algal bloom, which usually lasted for fewer than 2 months from outbreak to the ending of the algal bloom process. We can see that the algal blooms occurred frequently from May to September (the summer season in China), so we concentrated on studying the dynamics process of the algal bloom in the tributary (Ji et al., 2010; Liu et al., 2012). At the other side, we have to admit the insufficient frequency during the long-time field observation because of the huge observation workload in so many observation points and the difficulties caused by the steep slope in the reservoir. Meanwhile, some researchers used one year or longer observation data to validate their models, and they used the 1-dimensional or lateral-averaged 2-dimensional water quality model like CE-QUAL-W2 model (Ma et al., 2015). The position of plunge point and the intrusion thickness between the tributary and the Yangtze mainstream had to be set-up empirically (Ma et al., 2015), which will affect the modeling accuracy of the water quality process in the tributary, and in this way the local helical flow and vortexes near the river mouth of the several tributaries cannot be modeled like that shown in Fig. 4. Therefore, comprehensively considering the available field data and the computational scale, the population of observation data and the high-resolution simulation can reflect the characteristics of the flow field and water quality in the TGR mainstream and the tributaries.

The vertical distribution of phytoplankton biomass was mainly controlled by the underwater light intensity, which was generated by both of the shortwave and long wave solar irradiance. The underwater light intensity decayed quickly with water depth because of light attenuation by water background, suspended sediment, and the phytoplankton self-shading effect, which caused the vertical distribution difference of phytoplankton biomass as shown in Fig. 8. The calculated chlorophyll-a concentration agreed well with the sampled data at

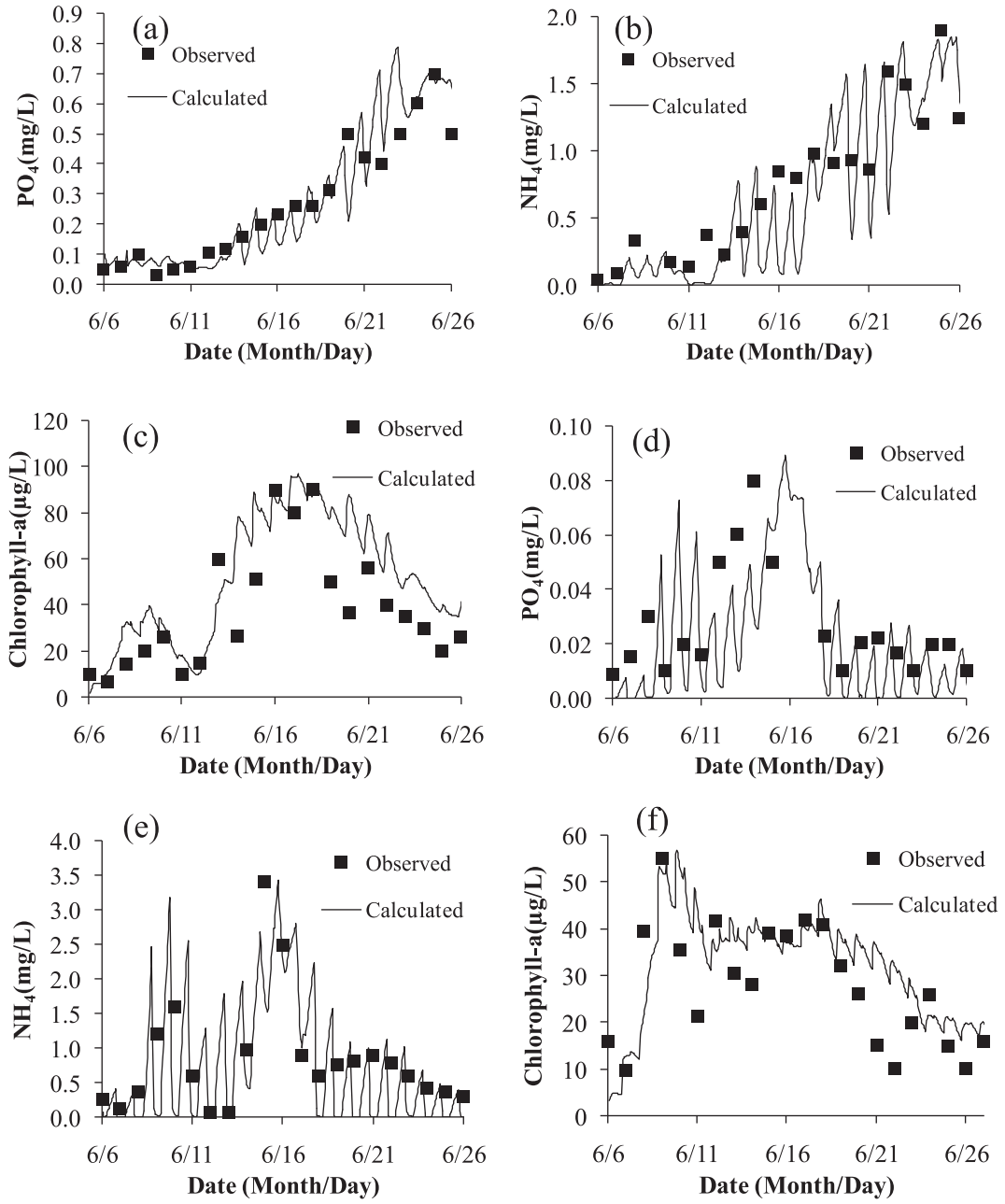

Fig. 9. The observed and calculated concentrations of nutrients and chlorophyll-a from June 10th to July 3rd, 2008 ((a) PO_4 at Gaoyang; (b) NH_4 at Gaoyang; (c) chlorophyll-a at Gaoyang; (d) PO_4 at Xiakou; (e) NH_4 at Xiakou; and (f) chlorophyll-a at Xiakou).

Xiakou, which reflected the quick growth of phytoplankton near the water surface and then decreased to nearly zero under 10 m depth because of the insufficient light. Moreover, the maximum chlorophyll-a concentration appeared about 1 m under the water surface (Fig. 8), which indicated the oversaturated light intensity at the water surface limited the growth of phytoplankton. The phenomenon cannot be observed by field observation because of the insufficient sampling points set in the water depth direction.

Some parameters that were mainly related with the newly added formulations and modules in EWASP (listed in Table 1) were calibrated for reproducing the dynamic changing process of nutrients and chlorophyll-a concentration. Other parameters in the coupled modeling used the default value in the literatures (Wool et al., 2008; Justic and Wang, 2014). The relative error of the calibrated results including nutrients and chlorophyll were all greater than 0.6 and the error analyses for the XXR can be found in previous literatures (Li et al., 2012, 2014).

3.4. Prediction

The calibrated SELFE-EWASP model was used to predict the algal bloom from June 10th to July 3rd, 2008, which can be verified by the available field data. Overall, the fluctuation of nutrients and chlorophyll-a showed diurnal changes that were similar to those indicated in the calibration period (Fig. 9). However, the concentrations of PO_4 and NH_4 at the water surface increased to 0.6 and 1.8 mg/L, respectively, at Gaoyang (Fig. 9(a) and (b)). The concentrations of PO_4 and NH_4 both reached maximum at June 20th, 2008 at Xiakou (Fig. 9(d) and (e)). The nutrients were affected by the diurnal change of phytoplankton near the water surface, but the nutrients in the deep-water zone were mainly determined by flow transport and chemical reactions. The maximum chlorophyll-a concentration occurred on June 23rd at Gaoyang and on June 16th, 2008 at Xiakou (Fig. 9(c) and (f)). The different transport process and the algal bloom occurring time showed that the water

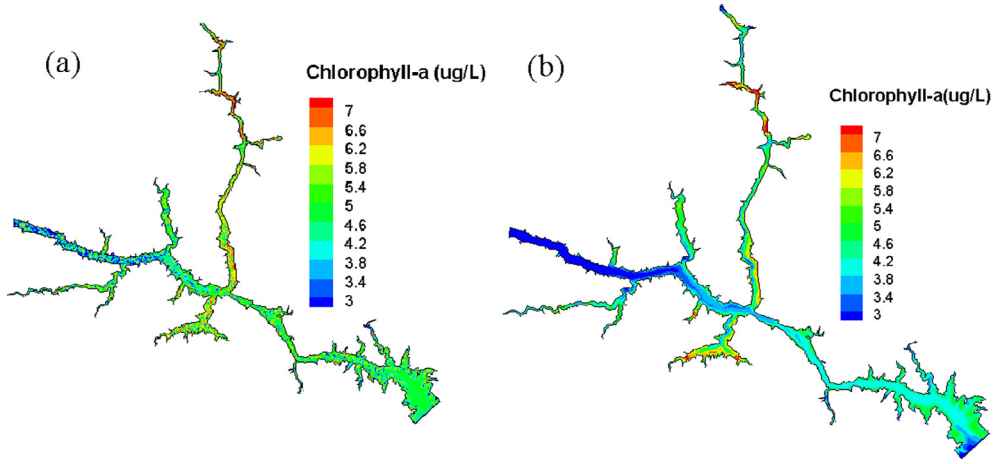

Fig. 10. The plane distribution of chlorophyll-a concentration at September 28th, 2007 ((a) near water surface and (b) near river bed).

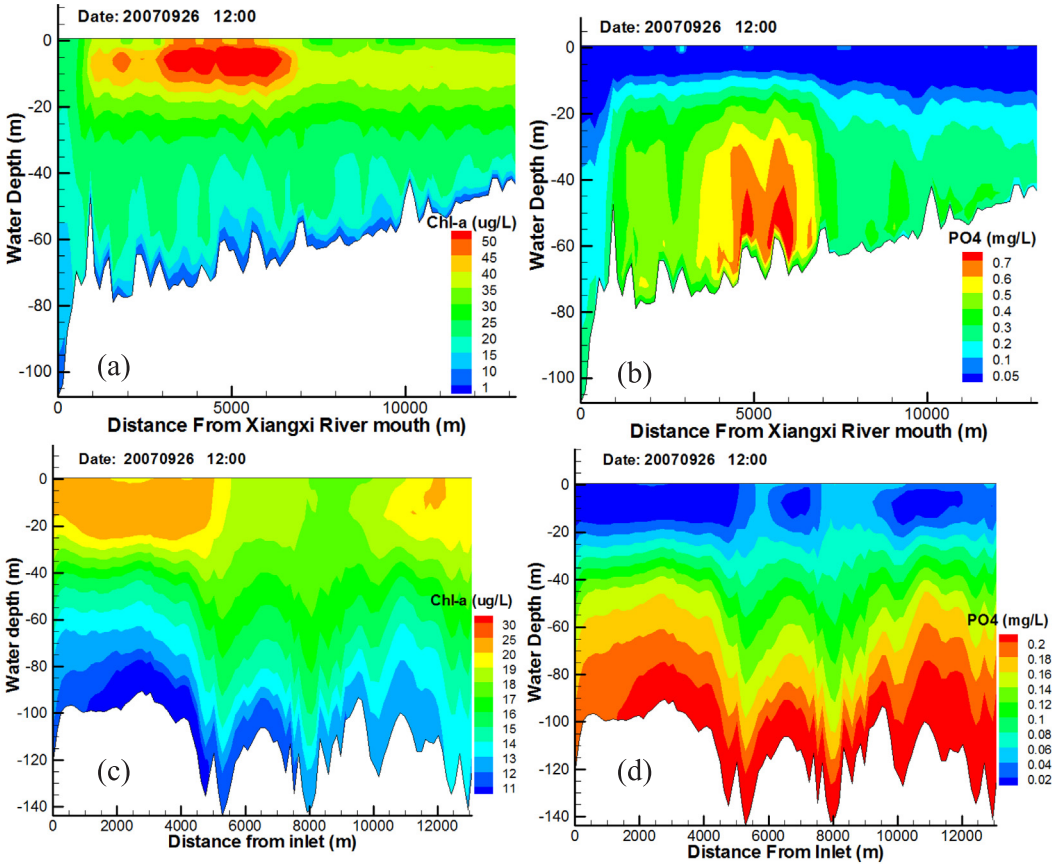

Fig. 11. The vertical distribution of PO_4 and chlorophyll-a concentration (vertical size exaggerated by 10 times) ((a) PO_4 in XXR; (b) chlorophyll-a in XXR; (c) PO_4 in the mainstream; and (d) chlorophyll-a in the mainstream).

quality in the XXR was much more controlled by the local pollutant load. The calculated results agreed well with the observed nutrients and chlorophyll-a, which indicated that the calibrated coupled model can spatially and temporally reproduce the dynamic process of the algal bloom in TGR.

The algal bloom can be diagnosed in most of the tributaries, especially in XXR, through observing the plane distribution of chlorophyll-a concentration in Fig. 10. The most serious algal bloom occurrences located at the middle reach of XXR in Fig. 10(a), which was consistent with the field observation and the position of the backwater tail as shown in Fig. 4(a). Moreover, the chlorophyll-a concentration near the bed showed less difference compared with that near water surface in the shallow water zone (Fig. 10(a)), while obvious difference can be seen in deep water (Fig. 10(b)) because the decayed underwater light intensity cannot support the growth of phytoplankton in deep water.

The vertical distribution of PO_4 and chlorophyll-a concentration in the XXR both showed clear stratification in Fig. 11(a) and (b), but there were no clear differences in the Yangtze River mainstream (Fig. 11(c) and (d)). The vertical distribution of chlorophyll-a and PO_4 concentration on September 26th, 2007 showed the higher concentration of chlorophyll-a and lower concentration of PO_4 presented near the water surface because of the active photosynthesis and the PO_4 adsorbed by the growth of phytoplankton (Fig. 11(b) and (d)). However, the chlorophyll-a concentration in the XXR reached a maximum of

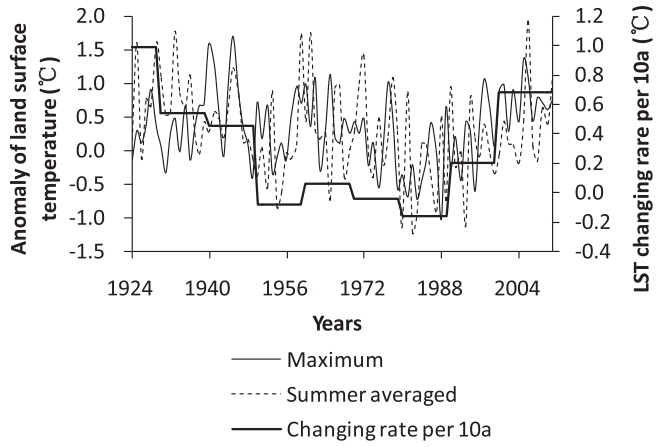

Fig. 12. The anomaly of land surface temperature at Yichang Station from 1924 to 2011.

50 μg/L, which was higher than that in the mainstream (less than20 μg/L) as shown in Fig. 11(a) and (c). Moreover, the PO_4 concentration near the bed was relatively high after considering the nutrients exchange with the bed sediment and released from the re-suspended sediment when the bottom shear stress reached the critical shear stress.

4. Discussions

The operation of the TGR affected the water quality, especially the water level fluctuation, the discharge and the pollutant load into the tributaries in the short term, which has been previously studied by numerical simulation and sensitivity analyses (Dai et al., 2013; Li et al., 2014; Ma et al., 2015; Huang et al., 2015a,b). Over the long term, the climate change and global warming trend reported by the Intergovernmental Panel on Climate Change (IPCC) (http://www.ipcc.ch/report/ar5/syr/) could affect the physical or chemical processes in the TGR. Some researchers have previously investigated the climate changes affecting the algal bloom and virus through changing the water temperature (Trolle et al., 2014; Vilhena et al., 2010; Wang et al., 2012). In this study, the coupled SELFE-EWASP model was used to assess the effect of the increased land surface temperature (LST) under the global warming background on the water quality in the TGR.

The LST at Yichang station was continuously recorded from 1924 to 2011, which was downloaded from China Meteorological Data Shared Service Center (http://data.cma.cn/data/). The anomaly of the maximum and the summer (from June to September) averaged LST showed that the anomaly was greater than 0 ℃ except the years from 1974 to 1995 as seen in Fig. 12. The obvious warming phenomenon can be observed before 50 s in the 20th century and the LST increasing rate reached 0.4 ℃/10a–0.9 ℃/10a and the LST increasing rate kept around 0.7 ℃/10a in the 21st century in Fig. 12, so the relative increased rate was 2%–5% per 10a. The high LST caused the surface water temperature increase and provided the favorable condition for the growth of the blue-green algae in the TGR (Ye et al., 2006; Xu et al., 2009), so the LST as the input of EWASP was decreased by 2%, 5%, and 10% of the LST used in the calibrated simulation (the base scenario) which were called Scenario-1, Scenario-2 and Scenario-3, respectively in Fig. 12. Then, the effect on the chlorophyll-a concentration at Gaoyang, Xiakou in the XXR and CJ04 in the mainstream was observed. All the initial and boundary conditions were the same as the calibrated simulation in Section 3.3.

The chlorophyll-a concentration at Gaoyang increased in the whole simulation period and reached the maximum value 70 μg/L after 15 days and there's no obvious difference among Scenario-1, Scenario-2 and Scenario-3 before the 12th day but the concentration difference of chlorophyll-a can reach 5 μg/L after the 12th day as seen in Fig. 13(a).

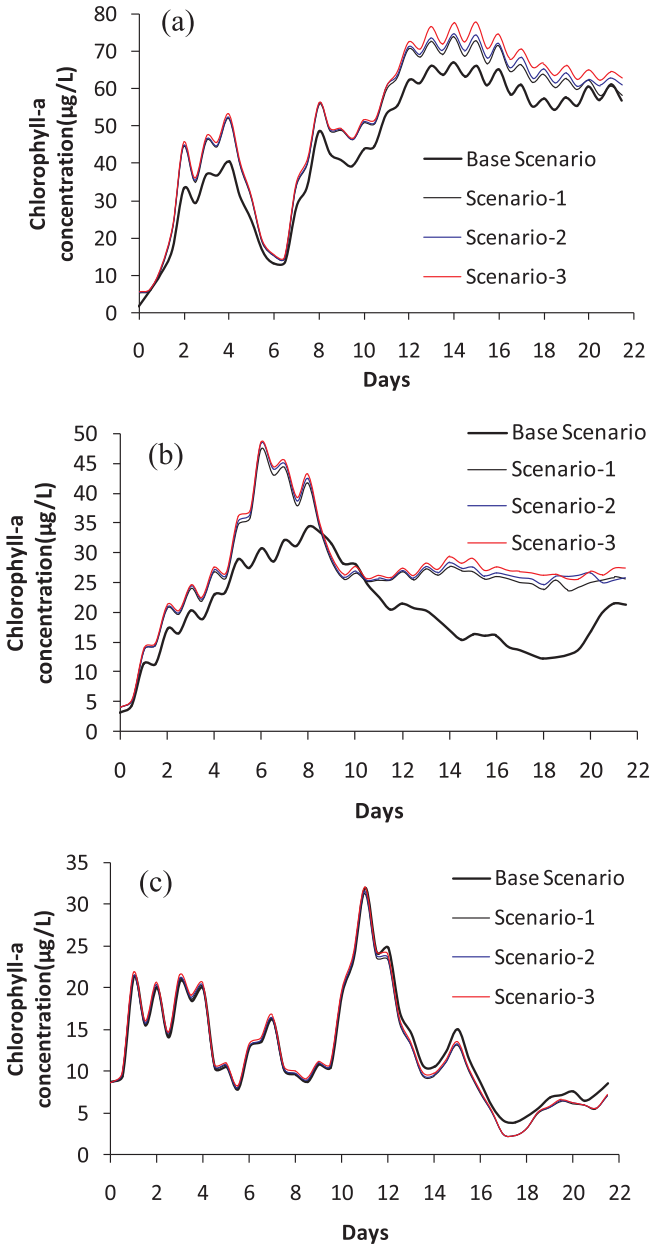

Fig. 13. The effect of LST on the chlorophyll-a concentration ((a) Gaoyang; (b) Xiakou; and (c) CJ04).

The concentration of chlorophyll-an at Xiakou reached the maximum value 50 μg/L at the 6th day which was greater than the maximum 30 μg/L at the 8th day, which indicated the increased LST made the peaking time 2 days in advance at Xiakou in Fig. 13(b) and leaded to the continued high concentration (25 μg/L) after 12 days compared with the decreased concentration from 25 μg/L to 10 μg/L in the base scenario. There's no obvious chlorophyll-a concentration difference at CJ04 point in the Yangtze River mainstream before the 14th day and the increased LST decreased the chlorophyll-a concentration after the 14th day to the very limited extent in Fig. 13(c). The different effects between the tributaries and the Yangtze River mainstream indicated that the thermal structure in the tributaries where the flow velocity was very low (less than0.01 m/s) affected the algal growth more obviously than that in the mainstream where the relatively high flowing transport capability can inhibit the algal bloom problem. There are cascaded reservoirs in the upstream of the Xiangxi River that intercepted considerable amount of water and sediment (Hormann et al., 2009), so the

cold water released from the cascaded reservoirs can inhibit the algal bloom in the upper and middle reach of XXR (Xu et al., 2009), of which the mechanism can be explained from the inverse process of the scenarios. Meanwhile, the released flush water generally accompanied with relative high suspended sediment concentration will also increase the light attenuation underwater and can inhibit the algal bloom in short time (Li et al., 2014).

5. Conclusions

A 3-dimensioal unstructured-mesh hydrodynamic model SEFLE has been coupled with a water quality model WASP and a biogeochemical model CANDI, and the coupled model was applied to study the sediment-related water quality process in the TGR. Some conclusions can be obtained using the coupled model as following:

(1) The vortex existed at the confluence of the tributaries and the Yangtze River mainstream was identified through the high-resolution modeling, and the opposite flow direction near the water surface and the river bed affected the nutrients and phytoplankton exchange between the tributaries and the mainstream.
(2) The extended version of WASP considered the processes included the DO exchange between the air and the water induced by the high flow velocity, the nutrients adsorbed by the suspended sediment particles, the nutrients exchange between the overlying water and the bed sediment and the diurnal solar radiance affecting the photosynthesis of phytoplankton can enhance the ability to reproduce the dynamic process of the algal bloom in TGR more accurately than the WASP6.0.
(3) The land surface temperature increased under the global warming background affected the ecosystem in the tributaries which increased the risk probability of the algal bloom, and the cold water released from the cascaded reservoirs in the upstream of Xiangxi River was suggested to inhibit the algal bloom in the downstream.

The coupled model developed in this study provided a promising tool for water quality assessment, prediction and management in lakes, rivers and coasts with complex boundary geometry. But the defects of the research should be pointed out that the large computation scale caused by the high-resolution 3-dimensional simulation limited the time length of the unsteady process which cannot reflect the seasonal variation of the nutrients and phytoplankton biomass in TGR and also the biogeochemical process in the bed sediment was still not clearly understood and calibrated, these problems should be solved through the parallelization computation and more field sampling in the future study.

Acknowledgements

This paper was supported by the National Key Research and Development Program of China (No. 2017YFC1404700) and the Open Fund of Key Laboratory of Sediment Research affiliated to the Yellow River Institute of Hydraulic Research (2015003). The authors are also grateful to the Xiangxi River Ecological Observation Station of Three Gorges University, China for providing the field data.

References

Ben, H., Chris, D., 2015. Estuary, Lake and Coastal Ocean Model: ELCOM v3.0 User Manual. Centre for Water Research University of Western Australia.
Chao, X.B., Jia, Y.F., Shields, F.D., et al., 2007. Numerical modeling of water quality and sediment related processes. Ecol. Model. 201 (3), 385–397.
Chu, C.R., Jirka, G.H., 2003. Wind and stream flow induced reaeration. J. Environ. Eng. (ASCE) 129 (12), 1129–1136.
Dai, H.C., Mao, J.Q., Jiang, D.G., et al., 2013. Longitudinal hydrodynamic characteristics in reservoir tributary embayments and effects on algal blooms. Plos One 8 (7), 1–14.
Ferziger, J.H., Peric, M., 2002. Computational Methods for Fluid Dynamics, 3rd edition. Springer-Verlag, Germany.
Hipsey, M.R., 2015. Computational Aquatic Ecosystem Dynamics Model: CAEDYM v3 User Guide. Centre for Water Research University of Western Australia.
Hormann, G., Koplin, N., Cai, Q., et al., 2009. Using a simple model as a tool to parameterise the SWAT model of the Xiangxi river in China. Quat. Int. 208 (1), 116–120.
Huang, L., Fang, H.W., Reible, D., 2015a. Mathematical model for interactions and transport of phosphorus and sediment in the Three Gorges Reservoir. Water Res. 85, 393–403.
Huang, L., Fang, H.W., Fazeli, M., et al., 2015b. Mobility of phosphorus induced by sediment resuspension in the Three Gorges Reservoir by flume experiment. Chemosphere 134, 374–379.
Ji, D.B., Liu, D.F., Yang, Z., 2010. Hydrodynamic characteristics of Xiangxi Bay in Three Gorges Reservoir. Scientia Sinica Physica: Mechanica & Astromica 40 (1), 101–112.
Jia, D.D., Shao, X.J., Zhang, X.N., et al., 2013. Sedimentation patterns of fine-grained particles in the dam area of the Three Gorges Project: 3D numerical simulation. J. Hydraul. Eng. (ASCE) 139 (1), 669–674.
Justic, D., Wang, L.X., 2014. Assessing temporal and spatial variability of hypoxia over the inner Louisiana-upper Texas shelf: application of an unstructured-grid three-dimensional coupled hydrodynamic-water quality model. Cont. Shelf Res. 72 (1), 163–179.
Li, J., Jin, Z.W., Yang, W.J., 2014. Numerical modeling of the Xiangxi River algal bloom and sediment-related process in China. Ecol. Inf. 22 (1), 23–35.
Li, J., Li, D.X., Wang, X.K., 2012. Three-dimensional unstructured-mesh eutrophication model and its application to the Xiangxi River, China. J. Environ. Sci. 24 (1), 1569–1578.
Li, W.J., Wang, J., Yang, S.F., et al., 2015. Determining the existence of the fine sediment flocculation in the Three Gorges Reservoir. J. Hydraul. Eng. (ASCE) 141 (2), 1–8.
Liu, L., Liu, D.F., Johnson, D.M., et al., 2012. Effects of vertical mixing on phytoplankton blooms in Xiangxi Bay of Three Gorges Reservoir: implications for management. Water Res. 46, 2121–2130.
Luff, R., Moll, A., 2004. Seasonal dynamics of the North Sea sediments using a three-dimensional coupled sediment-water model system. Cont. Shelf Res. 24 (10), 1099–1127.
Ma, J., Liu, D.F., Wells, S.A., et al., 2015. Modeling density currents in a typical tributary of the Three Gorges Reservoir, China. Ecol. Model. 296, 113–125.
Stone, R., 2008. Three Gorges Dam: into the unknown. Science 321, 628–632.
Trolle, D., Elliott, J.A., Mooij, W.M., et al., 2014. Advancing projections of phytoplankton responses to climate change through ensemble modelling. Environ. Modell. Softw. 61 (C), 371–379.
Vilhena, L.C., Hillmer, I., Imberger, J., 2010. The role of climate change in the occurrence of algal blooms: Lake Burragorang, Australia. Limnol. Oceanogr. 55 (3), 1188–1200.
Wang, C.F., Wang, H.V., Kuo, A.Y., 2008. Mass Conservative Transport Scheme for the Application of the ELCIRC Model to Water Quality Computation. J. Hydraul. Eng. (ASCE) 134 (8), 1166–1171.
Wang, L.L., Yu, Z.Z., Dai, H.C., et al., 2009. Eutrophication model for river-type reservoir tributaries and its applications. Water Sci. Eng. 2 (1), 16–24.
Wang, S., Qian, X., Han, B.P., et al., 2012. Effects of local climate and hydrological conditions on the thermal regime of a reservoir at Tropic of Cancer, in southern China. Water Res. 46 (8), 2591–2604.
Wool, T.A., Robert, B.A., James, L.M., et al., 2008. Water Quality Analysis Simulation Program (WASP) Version 6.0: User's Manual. US Environmental Protection Agency.
Xu, Y.Y., Cai, Q.H., Shao, M.L., et al., 2009. Seasonal dynamics of suspended solids in a giant subtropical reservoir (China) in relation to internal processes and hydrological features. Quat. Int. 208 (1), 138–144.
Yang, Z.J., Liu, D.F., Ji, D.B., et al., 2010. Influence of the impounding process of the Three Gorges Reservoir up to water level 172.5m on water eutrophication in the Xiangxi Bay. Sci. China (Technol. Sci.) 53(1), 1114–1125.
Ye, F., Zhang, Y., Friedrichs, M., et al., 2016. A 3D, cross-scale, baroclinic model with implicit vertical transport for the Upper Chesapeake Bay and its tributaries. Ocean Model. 107 (1), 82–96.
Ye, L., Xu, Y.Y., Han, X.Q., et al., 2006. Daily dynamics of nutrients and chlorophyll a during a spring phytoplankton bloom in Xiangxi Bay of the Three Gorges Reservoir. J. Freshwater Ecol. 21 (2), 315–321.
Zeng, X.B., Zhao, M., Dickinson, R.E., 1998. Intercomparison of bulk aerodynamic algorithms for the computation of sea surface fluxes using TOGA COARE and TAO data. J. Clim. 11 (11), 2628–2644.
Zhang, Y., Ye, F., Stanev, E.V., 2016. Seamless cross-scale modeling with SCHISM. Ocean Model. 102, 64–81.
Zhang, Y.L., Baptista, A.M., 2008. SELFE: A semi-implicit Eulerian-Lagrangian finite-element model for cross-scale ocean circulation. Ocean Modeling 21 (3), 71–96.
Zheng, T.G., Mao, J.Q., Dai, H.C., et al., 2011. Impacts of water release operations on algal blooms in a tributary bay of Three Gorges Reservoir. Sci. China (Technol. Sci.) 54(6), 1588–1598.
Zhou, J.J., Zhang, M., Lin, B.L., et al., 2015. Lowland fluvial phosphorus altered by dams. Water Resour. Res. 51, 2211–2226.